

Air-quality in the mid-21st century for the city of Paris under two climate scenarios; from regional to local scale.

K. Markakis¹, M. Valari¹, A. Colette², O. Sanchez³, O. Perrussel³, C. Honore³, R. Vautard⁴, Z. Klimont⁵, S. Rao⁵.

[1] {Laboratoire de Meteorologie Dynamique, IPSL Laboratoire CEA/CNRS/UVSQ, Ecole Polytechnique, 91128 Palaiseau Cedex, France}

[2] {Institut national de l'environnement industriel et des risques (INERIS), Paris, France}

[3] {AIRPARIF}

[4] {Laboratoire des Sciences du Climat et de l'Environnement, IPSL Laboratoire CEA/CNRS/UVSQ, Orme des Merisiers, F-91191 Gif/Yvette Cedex, France}

[5] {International Institute for Applied Systems Analysis, Schlossplatz 1, 2361, Laxenburg, Austria}

Correspondence to: K. Markakis (konstantinos.markakis@lmd.polytechnique.fr)

Abstract

Ozone and PM_{2.5} concentrations over the city of Paris are modeled with the CHIMERE air-quality model at 4km x 4km horizontal resolution for two future emission scenarios. A high resolution (1x1 km) emission projection until 2020 for the greater Paris region is developed by local experts (AIRPARIF) and is further extended to year 2050 based on regional scale emission projections developed by the Global Energy Assessment. Model evaluation is performed based on a 10-year control simulation. Ozone is in very good agreement with measurements while PM_{2.5} is underestimated by 20% over the urban area mainly due to a large wet bias in wintertime precipitation. A significant increase of maximum ozone relative to present time levels over Paris is modeled under the “business as usual” scenario (+7 ppb) while a more optimistic mitigation scenario leads to moderate ozone decrease (-3.5 ppb) in year 2050. These results are substantially different to previous regional scale projections where 2050 ozone is found to decrease under both future scenarios. A sensitivity analysis showed that this difference is due to the fact that ozone formation over Paris at the current, urban scale study, is driven by VOC-limited chemistry, whereas at the regional scale ozone formation occurs under NO_x-sensitive conditions. This

1 explains why the sharp NO_x reductions implemented in the future scenarios have a different
2 effect on ozone projections at different scales. In rural areas projections at both scales yield
3 similar results showing that the longer time-scale processes of emission transport and ozone
4 formation are less sensitive to model resolution. PM_{2.5} concentrations decrease by 78% and 89%
5 under “business as usual” and “mitigation” scenarios respectively compared to present time
6 period. The reduction is much more prominent over the urban part of the domain due to the
7 effective reductions of road transport and residential emissions resulting in the smoothing of the
8 large urban increment modelled in the control simulation.

9

10 **1 Introduction**

11 Climate change can affect air quality through a number of mechanisms related to meteorological
12 variables such as temperature, humidity, precipitation, solar radiation, wind speed and the
13 planetary boundary layer height. If the effects of atmospheric pollutants (greenhouse gasses,
14 other gaseous species and aerosols) on climate change have been extensively investigated over
15 the last decades (IPCC, 2001, 2007) the impact of these emissions and changed climate on air
16 quality has only raised interest during the last few years and many issues remain open. Most of
17 these studies use global chemistry-transport models (CTMs) to study the impact of changing
18 climate on tropospheric ozone at either global (Brasseur et al., 1998; Liao et al., 2006; Prather et
19 al., 2003; Szopa and Hauglustaine, 2007) or regional scale (Murazaki and Hess, 2006; Szopa et
20 al., 2006). The resolution of these studies, typically a few hundreds of kilometers, is insufficient
21 to capture the high spatial variability of air pollution due to the short lifetime of tropospheric
22 ozone and particulate matter (in the range of some hours up to a few days) (Seinfeld and Pandis,
23 2006) as well as to the sharp horizontal gradients of anthropogenic emissions over urban areas.
24 Moreover, the chemistry-climate models used in such large-scale studies suffer from a simplistic
25 representation of regional scale chemistry.

26 Only few, recent, applications study the impact of changing climate on air quality using regional
27 CTMs. These models include more sophisticated chemistry at typical resolutions of tenths of
28 kilometers and therefore provide a better understanding of the underlying mechanisms at
29 regional scale. The first documented modeling study on the impact of future conditions at
30 regional scale is that of Hogrefe et al. (2004) while at the same time Knowlton et al. (2004) took
31 a step forward and performed a health impact assessment study for the greater New York region.

1 Since then several researchers performed similar regional applications in order to derive future
2 predictions of ozone and/or aerosols using offline climate-chemistry models (Colette et al., 2013;
3 Kelly et al., 2012; Lam et al., 2011; Langner et al., 2005; Nolte et al., 2008; Steiner et al., 2006;
4 Szopa and Hauglustaine, 2007; Tagaris et al., 2009), on-line climate-chemistry models (Forkel
5 and Knoche, 2006, 2007) or multi-model studies (Colette et al., 2012; Langner et al., 2012).

6 An open research challenge today is the impact of climate change on air-quality at urban scale.
7 Enhanced health effects due to increasing urbanization (UNFPA, 2007) should be addressed
8 primarily at such scale especially given that the efforts to mitigate air-pollution are more intense
9 in areas where the largest health benefits are observed (Riahi et al., 2011). The common
10 approach to study the effects of climate change and emissions at city level is to use regional scale
11 CTMs. However the resolution of current model studies remains too coarse to represent the high
12 spatiotemporal variability of pollutants at urban scale. Regional scale emission inventories fail to
13 represent the plethora of emission activities in terms of e.g. the underlying technologies used
14 within a specific source sector or to take into account the habitual patterns of the population at
15 large cities (Markakis et al., 2010, 2012). The substantial part of the published work uses
16 emission projections based on scenarios developed to represent changes at global scale and are
17 rarely well suited for local scale assessment e.g. they lack the detailed representation of all
18 emission activities at a finer scale. For example, the more recent Representative Concentration
19 Pathways (RCPs) (van Vuuren et al., 2011) developed to support modeling activities for the new
20 assessment of the Intergovernmental Panel on Climate Change (IPCC) incorporate a diversity of
21 radiative forcing scenarios that may be suitable for large scale chemistry-climate models but not
22 appropriate to represent emission trends for specific cities and therefore regional scale air-quality
23 assessment (Butler et al., 2012). Grid resolution is another key issue for urban scale modeling as
24 shown by previous research (Arunachalam et al., 2006; Cohan et al., 2006; Valari and Menut,
25 2008). The assumption of instantaneous mixing of emissions within the volume of the regional
26 scale CTMs' grid cells is unsuitable to represent local scale chemistry (such as ozone titration)
27 when the grid-cell size is too large compared to the actual size of the emitting areas. It has been
28 shown previously that use of coarse resolution leads to underprediction of daily ozone maxima
29 and to overprediction of daily average ozone levels (Arunachalam et al., 2006; Tie et al., 2010;
30 Vautard et al., 2007). Valin et al. (2011) show that grid resolution finer than ~10 km is often
31 necessary to capture ozone chemistry near areas with large NO_x emissions. Due to the non-

1 linearity of ozone chemistry the inability of large grid sizes to differentiate urban and rural areas
2 can have a profound effect on the simulated ozone concentrations (Silman et al., 1990). Forkel
3 and Knoche (2007) found that the increase of future maximum ozone concentrations in Europe
4 occurred in areas where high mixing ratios of NO_x coincided with increased isoprene emissions,
5 indicating that the failure of coarser resolutions to efficiently distinguish between urban and rural
6 areas would result in overestimation of future ozone in cities near to high isoprene emitting
7 sources. The current challenge is to develop realistic long-term emission projections at a city-
8 scale and bridge the gap between local, regional and global scale modeling.

9 The aim of our study is to develop mid-21st century horizon air quality projections over the
10 greater Paris area under two consistent emission and climate scenarios (10-year continuous
11 simulation). To the authors knowledge this is the first time where a 10-year air-quality projection
12 under climate and city level emission changes has been conducted at urban scale and resolution
13 as fine as 4 km. Local emission projections used in this study are compiled by merging several
14 pieces of information: i) a high resolution (i.e. 1 km) city specific emission inventory developed
15 by AIRPARIF (present time emissions); ii) a city-scale short-term projection (until 2020)
16 considering air-quality policies already in place and planned for the city for the next years iii)
17 two mid-21st century regional scale emission scenarios including both climate and regional air
18 quality policies developed by the Global Energy Assessment (GEA) (Riahi et al., 2012). The
19 “reference” (REF) scenario is consistent with long-term climate outcomes of the RCP-8.5
20 adopting all current and planned air quality legislation until 2030 and assumes that no climate
21 policies are implemented thereafter. The “mitigation” (MIT) scenario is consistent with long-
22 term climate outcomes of the RCP-2.6 and additionally assumes stringent climate mitigation
23 policies. The final fine scale, mid-21st horizon emission inventory for the greater Paris area, the
24 Ile-de-France region (IdF), was obtained by scaling the 2020 high resolution emission inventory
25 to the year 2050 using the regional scale GEA scenarios.

26 After describing the methodology in Section 2, an evaluation of the modelling system is
27 described in Section 3 and scenario results are presented in Section 4. Our conclusions are
28 discussed in Section 5.

29

30 **2 Materials and methods**

1 The Ile-de-France region (IdF) is located at 1.25–3.58° east and 47.89–49.45° north with a
2 population of approximately 11.7 million, more than two million of which live in the city of
3 Paris (Fig. 1). The area is situated away from the coast and is characterized by uniform and low
4 topography, not exceeding 200 m above sea level.

5 An “off-line” modeling approach is used to assess air-quality in the study region as a response to
6 climate and emission changes. For both climate and air-quality simulations we use a dynamical
7 downscaling approach consisting of two one-way nesting steps: from global to regional scale
8 over Europe and from regional to local scale over the IdF region. IPSL-CM5A-MR global
9 circulation model (Dufresne et al., 2013) is used to derive future projections of the main climate
10 drivers (temperature, solar radiation etc.) using a set of available global greenhouse gas emission
11 scenarios (RCP-2.6 and RCP-8.5). Global climate output is downscaled with the Weather
12 Research and Forecasting (WRF) mesoscale climate model (Skamarock and Klemp, 2008) at two
13 steps: first over a 50km resolution grid over Europe and then on a 10 km resolution grid over
14 France using one-way nesting. We drive the CTM over IdF using the 10km meteorology
15 acknowledging the fact that higher resolution meteorology could have an impact in modelled
16 pollutant concentrations. However, due to the geographical characteristics of the greater Paris
17 area (flat topography at great distance from any mountains or the ocean) and as shown in
18 previous studies over the same region using the CHIMERE CTM (Menut et al., 2005a; Valari
19 and Menut., 2008) increasing the resolution of the meteorological input does not improve the
20 results of the chemistry-transport modelling. More specifically, Menut et al. (2005a) showed that
21 apart from coastal areas where refined meteorology improved air-quality modelling results, in
22 the rest of France ozone peaks were better captured with lower resolution meteorological input.
23 Valari and Menut (2008) showed that a refined meteorological input gives similar results for
24 ozone and that model performance is much more sensitive to the resolution of emissions than to
25 meteorology.

26 Air-quality data are downscaled with the CHIMERE model (Menut et al., 2013) a detailed
27 description of which can be found at: <http://www.lmd.polytechnique.fr/chimere>. CHIMERE is an
28 off-line chemistry-transport model (CTM), which models atmospheric chemistry and transport,
29 forced by anthropogenic emissions, biogenic emissions, a meteorological simulation and
30 boundary conditions. It is a cartesian-mesh grid model including gas-phase, solid-phase and
31 aqueous chemistry, biogenic emissions modeling depending on meteorology with the MEGAN

1 model (Guenther et al., 2006), dust emissions (Menut et al., 2005b) and resuspension (Vautard et
2 al., 2005). Gas-phase chemistry is based on the MELCHIOR mechanism (Lattuati, 1997) which
3 includes more than 300 reactions of 80 gaseous species. The aerosols model species are sulfates,
4 nitrates, ammonium, organic and black carbon and sea-salt (Bessagnet et al., 2010) and the gas-
5 particle partitioning of the ensemble Sulfate/Nitrate/Ammonium is treated by the ISORROPIA
6 code (Nenes et al., 1998) implemented on-line in CHIMERE.

7 Initial and boundary conditions are taken from global scale concentrations modelled with the
8 coupled LMDz-INCA global chemistry model (Hauglustaine et al., 2004; Szopa et al., 2012) and
9 are then downscaled with CHIMERE using two-level one-way nesting first at a 0.5° resolution
10 grid (~50 km) over Europe (Colette et al., 2013) and then at the 4km resolution grid over the IdF
11 region (local scale runs). For more details on the global and regional modeling exercises the
12 reader is referred to Hauglustaine et al. (2013) and Colette et al. (2013) respectively.

13 We performed three sets of 10-year runs at local scale: a continuous control run (CTL) from
14 1995 to 2004 representing present time air-quality and two continuous runs over the 2045-2054
15 decade representing air-quality projections to the mid-21st century horizon under two different
16 pathways of climate and emissions. To minimize the effect of inter-annual variability and
17 increase the statistical significance of model output longer term simulations should have been
18 performed. However, given the high resolution of the modeling exercise the computational cost
19 of longer simulations was considered too high for the present study.

20

21 **2.1 Models setup**

22 The modeling domain has a horizontal resolution of 4 km and consists of 39 grid cells in the
23 west-east direction and 32 grid cells in the north-south direction, thus covering a total region of
24 156 x 128 km². Twelve σ -p hybrid vertical layers were used to represent the atmospheric column
25 from the surface up to approximately 500hPa (~5.5 km) with the thickness of the first layer being
26 8 m. Simulations were performed with a time step of 5 minutes. Hourly meteorological fields
27 necessary for CHIMERE were modeled with WRF model v3.4. WRF simulations were carried
28 out on a 10 km resolution grid of 90x85 cells. Vertically the domain is divided into 31 σ -layers
29 extending up to 55hPa (~20 km). The time integration step was set to 1 minute. The physical
30 options used for these simulations are the WRF Single Moment 6-class microphysics scheme
31 (Hong and Lim, 2006), RRTM (rapid radiative transfer model) long-wave radiation scheme

1 (Mlawer et al., 1997), Dudhia short-wave radiation scheme (Dudhia, 1989), NOAH land surface
2 model (Chen and Dudhia, 2001), Asymmetric Convective Model version 2 Planetary Boundary
3 Layer scheme (Pleim, 2007) and Kain-Fritsch cumulus parameterization scheme (Kain, 2004).

4 5 **2.2 Data and metrics for model evaluation**

6 CHIMERE model evaluation has been performed in numerous studies at both regional (see e.g.
7 Solazzo et al., 2013a, 2013b and references therein) and urban scales (Hodzic et al., 2005;
8 Vautard et al., 2007). However, due to the climate component of the study our modeling setup
9 requires a different evaluation framework. We use 29 surface monitors of the local air-quality
10 network AIRPARIF classified as urban (17 sites), suburban (4 sites) and rural (8 sites). Only
11 monitoring sites with more than 70% of available data (hourly values) through the 10-year period
12 were considered for the evaluation process. Observations are conducted at a height ranging from
13 3 to 8m from the surface, which makes the first model layer concentrations directly comparable
14 with the observations.

15 Given that adverse health impact is mainly correlated to daytime ozone levels in the present
16 framework we focus on the evaluation of daytime and maximum ozone only. A variety of
17 metrics are used to evaluate model performance. For ozone the widely used mean normalized
18 bias (MNB) and mean normalized gross error (MNGE) are estimated. US EPA suggests that
19 MNB for modeled ozone concentrations should lie within the $\pm 15\%$ range and MNGE not
20 exceeding 35%. Regarding $PM_{2.5}$ the Mean Fractional Bias (MFB) and the Mean Fractional Error
21 (MFE) are used. A literature review of targeted range of values for fine particles can be found in
22 EPA (2007). The narrowest of the reported ranges suggests that for modeled $PM_{2.5}$ MFB should
23 fall within the $\pm 30\%$ range and MFE not exceeding 50%.

24 We extract these metrics from the daytime concentrations values and not the decade average
25 bearing in mind that this is not typical for runs forced by climate simulations but for operational
26 forecast evaluation. Here we do not use re-analyses to force the regional CTM but global and
27 regional climate simulations. Consequently one should expect lower scores than those yielded by
28 an air-quality forecast simulation, especially in the presence of climate biases (Colette et al.,
29 2013; Menut et al., 2013). Since this work is original in its concept we aim to evaluate whether
30 the urban scale setup is sufficiently realistic but utilizing metrics that are timely averaged on a
31 scale finer than a climatological one.

1
2
3
4
5
6
7
8
9
10
11
12
13
14
15
16
17
18
19
20
21
22
23
24
25
26
27
28
29
30
31

2.3 Climate and emission scenarios

Two long-term scenarios are used in the global-scale simulations of future climate conditions: RCP-8.5 and RCP-2.6. RCP-8.5 (Riahi et al., 2011) is a “reference” type scenario with no mitigation for greenhouse gases leading to a global radiative forcing of 8.5 W m^{-2} by the end of the century. RCP-2.6 (van Vuuren et al., 2011a) leads to a global radiative forcing of 2.6 W m^{-2} by the end of the century (2100), consistent with the goal of limiting the increase of global average temperature due to human activity to 2°C . Both RCP scenarios include century-long estimates of air pollutant emissions, including aerosols, and were used as input in the LMDz-INCA global chemistry model.

Present time emission estimates for the IdF region are available in hourly intervals, with a spatial resolution of $1 \times 1 \text{ km}$. The emission dataset was compiled by local experts using a variety of city-specific information integrating a number of anthropogenic activities in the IdF region (AIRPARIF, 2012). The spatial allocation of emissions is completed with proxies such as high-resolution population maps, road network and the location of industrial units. It includes emissions of CO , NO_x , Non-methane Volatile Organic Compounds (NMVOCs), SO_2 , PM_{10} and $\text{PM}_{2.5}$ with a monthly, weekly and diurnal (source specific) temporal resolution. The distribution of emissions among different activity sectors reveals that in the IdF region the principal emitter of NO_x , on annual basis, is the road transport sector (50%), for NMVOCs the use of solvents (46%) and for fine particles the residential sector (40%). Annual emissions rates within the simulated decade were kept constant; only the vertical distribution of point source emissions across model layers varies in time since it depends on several meteorological variables such as temperature and wind (plume-rise algorithm) (Scire et al., 1990). Finally the 1 km resolution emissions were aggregated to the 4 km resolution grid.

Mid-21st century (year 2050) emission projections for IdF incorporate local scale information, including the implementation of planned policies. The short-term component consists of the local scale 2020 emission projection compiled by AIRPARIF in the framework of the “Plan de Protection de l’Atmosphere d’Ile de France” (PPA) and with the support of the “Direction Regionale et Interdepartementale de l’Environnement et de l’Energie d’Ile de France” (DRIEE-IF). Emissions for 2020 correspond to a “business as usual” scenario assuming the implementation of all regulatory measures planned by the PPA.

1 The long-term component of the projection is established by linking two primary sources of
2 information: (i) the aforementioned 2020 AIRPARIF inventory and (ii) a set of scenarios from
3 the recently published Global Energy Assessment (GEA) (Riahi et al., 2012) to extend
4 projections until 2050. The GEA scenarios, while consistent with similar long-term climate
5 outcomes as the RCPs, include a more detailed representation of short-term air quality
6 legislations from the GAINS model (Amann et al., 2011). Outputs are based on the MESSAGE
7 model (Riahi et al., 2007) and include estimates of energy and greenhouse gas emissions for 11
8 global regions while air pollutants are further available at $0.5^\circ \times 0.5^\circ$ resolution estimated based
9 on inventory data described in Granier et al. (2011) and Lamarque et al. (2010) and an exposure-
10 driven algorithm for the downscaling of the regional air-pollutant emission projections. The
11 GEA scenarios have been used to estimate global health impacts of outdoor air pollution (Rao et
12 al., 2012, 2013) as well as for regional impacts analysis (Colette et al., 2012, 2013). Two GEA
13 scenarios are used in our analysis: i) a “reference” (REF) scenario (consistent with long-term
14 climate outcomes of the RCP-8.5) which adopts all current and planned air quality legislation
15 until 2030 and assumes that no climate policies are implemented thereafter ii) a “mitigation”
16 (MIT) scenario (consistent with long-term climate outcomes of the RCP-2.6) which additionally
17 assumes stringent climate mitigation policies consistent with a target of 2°C global warming by
18 the end of the century (2100). Thus the MIT scenario can be used to assess the co-benefits of
19 climate induced strategies. We derived national-wide annual totals (for France) in 2020 and 2050
20 for a number of pollutants from the GEA scenarios. 2050 over 2020 scaling ratios were
21 calculated for each pollutant for each source sector accounted for in the GEA dataset. The
22 resulting ratios are used as coefficients to scale the local 2020 AIRPARIF inventory without
23 modifying the spatial and temporal patterns.

24 We decided to derive scaling ratios based on national totals and not from the GEA 0.5° resolution
25 grid to avoid adopting the relatively simplistic approaches of the GEA downscaling algorithm for
26 the distribution of emissions at the finer scale. Thus, our approach benefits from the highly
27 resolved emission variability over Paris from the AIRPARIF inventory but it must be noted that
28 at the same time we inherently assume the energy transition over the 2020 to 2050 period
29 according to the REF and MIT scenarios. This is particularly relevant as the GEA scenarios
30 implement significant improvements in energy efficiency and a complete implementation and
31 continuation of air-quality policies in Europe. Thus we observe significant reductions in

1 emissions for the IdF region in 2050 (Table 1). While using different scenarios would lead to
2 alternative estimates of 2050 emissions, it is important to note that significant technological
3 change in the energy systems would likely mean that air pollutant emissions in Europe would
4 decline over the long-term in any case, although the exact distribution of such reductions is
5 uncertain.

6

8 **3 Model evaluation based on the control simulation (present time)**

9 **3.1 Meteorology**

10 It is beyond the purpose of this study to provide an in-depth meteorology evaluation, however to
11 build confidence in the meteorological fields used as input for our air-quality simulations we
12 present a short model evaluation based on the CTL run.

13 WRF meteorology for the CTL simulation ran over a 10 km resolution grid. Model results are
14 compared to surface observations from 7 meteorological stations found inside the IdF region.
15 Only one of these monitors (MONT) is actually inside the city of Paris. The mean wintertime
16 (DJF) and summertime (JJA) modeled and observed daily average values were calculated for 4
17 different variables relevant to air quality: 2m temperature, wind speed at 10m, relative humidity
18 and total precipitation (Table 2). A warm bias during summer reaches +0.8°C in the city center
19 (MONT station). This is bound to lead to enhanced ozone formation due to the thermal
20 decomposition of PAN releasing NO_x (Sillman and Samson, 1995). Modeled wind speeds are
21 higher than the observed ones both during winter and summer, a bias consistent with previous
22 studies (see e.g. Jimenez et al. (2012) for WRF or Vautard et al. (2012) for other models). This is
23 expected to enhance pollutants' dispersion and lead to less frequent stagnation episodes. The
24 model underestimates summertime relative humidity (bias=-13.3%). A systematic wet bias in
25 wintertime precipitation is observed in the city reaching +26.5%. This is expected to lead to
26 underestimation of PM levels through rain scavenging (Fiore et al., 2012).

27

28 **3.2 Ozone concentrations**

29 Scatter plots in Fig. 2 compare modeled ozone with surface measurements. Mean daytime
30 surface ozone and O_x (NO₂+O₃) (averaged over the April-August period) as well as the daily
31 maximum of 8-hour running means (MD8hr) from the urban stations are shown. Modeled
32 daytime ozone is in very good agreement with measurements over the urban cluster with a bias

1 of only +0.25 ppb (0.8% overestimation). Note that the spread of ozone bias among individual
2 stations is also small. O_x is often used as an indicator of ozone photochemical build-up because it
3 rules out titration process. Therefore, the low O_x bias indicates that local scale modeling
4 reproduces sufficiently both urban titration (daytime) and photochemical formation. NO_2 bias
5 (not shown) is also low (-0.32 ppb). Model results for ozone are considered satisfactory given the
6 nature of these runs (forced by climate simulations and not forecast meteorology as discussed in
7 Sect. 2.2). The MNB (+16.5%) and MNGE (+40.6%) are outside but near the US EPA targeted
8 ranges (+-15% and +35% respectively). For downtown Paris sites (not shown) MNB is +10.9%
9 and MNGE is equal to +39.8%. However, the model underestimates MD8hr by -7.8% (bias =-3.2
10 ppb). The 95th percentile (not shown) of observed and modeled ozone daily maxima differ by
11 13.8 ppb (-20.1%) indicating that the model fails to reproduce ozone levels under extreme
12 photochemical episodes. To some extent the high simulated winds produce milder stagnation
13 episodes and suppress ozone build-up (Jacob and Winner, 2009; Vautard et al., 2007); the
14 overestimation of wind speed leads to less frequent stagnation episodes (Sect. 3.1). On the same
15 time, the climate model suffers from a cold and overcast bias (Colette et al., 2013) that inhibits
16 the emission of biogenic precursors and ozone buildup.

17 Overestimation of mean daytime ozone is observed in all suburban and rural stations (+10.9%
18 and +11.3% respectively) even though O_x is in relatively good agreement with measurements.
19 This points to an underestimation of NO_2 and titration is represented less faithfully. Ozone
20 overestimation is due to some extent to the boundary conditions. This is supported by the fact
21 that both upwind and downwind rural stations show the same level of overestimation portraying
22 a spatially symmetric influence of boundary conditions (not shown). In the urban areas the strong
23 titration probably depletes the excess of ozone from the boundaries pointing to a possible
24 exaggeration of urban titration in the model. MNB and MNGE scores for suburban and rural
25 sites (Fig. 2) in general lie close but outside the US EPA targeted ranges.

26

27 **3.3 Fine particulate matter**

28 Modeled $PM_{2.5}$ surface concentrations are compared to all available measurements (i.e four
29 urban sites only one of which located in Paris). Results for wintertime (DJF), summertime (JJA)
30 and on annual basis are shown in Fig. 3. The model underestimates $PM_{2.5}$ by 20% in wintertime
31 (-14% at the Paris site). This underestimation could be attributed to the significant positive bias

1 in modeled precipitation and wind speeds (Sect. 3.1). Another explanation could be that the
2 monthly temporal profiles used to distribute the annual emissions of residential heating are based
3 on mean temperature variations. This could lead to strong underestimation of emissions in
4 wintertime. The analysis of the annual model results yields even higher underestimation for both
5 Paris site and domain-wide values (-18.9% and -26.6% respectively). The poorer model
6 performance during summertime suggests a possible underestimation of summertime emissions
7 in the local inventory. Vehicle-induced resuspension of particles might be a significant missing
8 source, especially during the drier summertime months (Schaap et al., 2009 and references
9 therein). PM_{2.5} underestimation, to some extent, is due to a poor representation of secondary
10 organic aerosol (SOA) in the model (modeled SOA concentrations are <0.5% in wintertime and
11 ~1.5% in summertime). This is a well-known shortcoming of regional CTMs (Simpson et al.,
12 2007; Solazzo et al., 2012; Stern et al., 2007). In particular Hodzic et al. (2009; 2010) found
13 significant underprediction of observed SOA concentrations modeled with CHIMERE in the
14 framework of the MILAGRO campaign. Modeled meteorology (wind and precipitation
15 overestimation) also contributes to the observed PM underestimation. The boundary layer height
16 is overestimated by 12% in the model leading to increased vertical diffusion and lower
17 concentrations. Overall, wintertime and annual metrics are within the US EPA targeted range
18 (MFB within +-30% and MFE <50%).

19

20 **3.4 Conclusions on model evaluation**

21 The model is able to represent the main features of ozone photochemical cycle (ozone formation
22 and titration) over the Ile-de-France region but fails to reproduce high ozone episodes. Urban
23 features of ozone chemistry, such as ozone titration are resolved showing that the emission
24 inventory is realistic. Therefore, this local scale modeling makes it possible to discern between
25 urban, suburban and rural areas and provides a good representation of both ozone build-up and
26 titration processes. The underestimation of PM_{2.5} is attributed to errors in modeled meteorology
27 (high precipitation and winds) and possibly to missing emission sources and chemical processes
28 (secondary organic aerosol).

29

30 **4 Future scenario analysis**

31 **4.1 Climate projections for the mid-21st century in Paris**

1 Table 3 summarizes the projections of key meteorological variables. It is beyond the scope of
2 this study to disentangle the effects of climate and emission changes on air-quality and therefore
3 only a brief qualitative discussion is provided in this section.

4 Under the REF scenario, which assumes that greenhouse gases increase monotonically until the
5 end of the century, the annual mean surface temperatures in the mid-21st horizon exhibits an
6 overall domain-wide increase of +1.1 °C (+1.0°C over the city) compare to the present time
7 period. Consequently, enhanced ozone formation is expected especially in the rural part of the
8 domain due to increase of biogenic organic compounds (BVOCs). Monoterpenes are especially
9 sensitive to temperature while isoprene to both temperature and sunlight. We do not observe any
10 significant changes to short-wave radiation, RH or precipitation under the REF scenario.

11 A -0.5°C decrease in the annual surface temperature compared to present time period is modeled
12 under the MIT trajectory, with two particularly cold years (2051 and 2052) lowering the decade
13 average. The inter-annual variability (standard deviation) is 2.54°C around a decade average of
14 11.3°C while under the REF scenario the variability is 0.8°C around a decade average of 13°C.
15 The internal natural variability of temperature can be very large at regional scale (Deser et al.,
16 2012), which stresses the need for longer simulation periods over which the inter-annual
17 variability would be smoothed. Lower temperatures are expected to inhibit ozone formation
18 while the drop of shortwave downward radiation by 16.6% relative to present will lead to less
19 BVOCs in the rural areas. We observe a significant increase in total precipitation compared to
20 the control simulation by a factor of 3.2 under the MIT pathway where, similarly to temperature,
21 two particularly wet years (2050 and 2051) are simulated. Modeled precipitation is high only on
22 a limited amount of days within those two years (standard deviation=0.73 around a decade
23 average of 0.32). In the regional simulation from which boundaries were utilized to force the
24 local runs, climate is also shown significantly wetter under MIT by a factor of 3.6.

25

26 **4.2 Ozone projections**

27 Mid-21st century ozone projections averaged over the April through August period are presented
28 in Fig. 4 for the REF and the MIT scenarios. Panel a shows present time MD8hr levels (CTL
29 simulation) whereas panels b and c provide differences between each of the REF and MIT
30 scenarios and the CTL simulation. The CTL simulation is able to dissociate the fast ozone
31 titration process from the longer scale photochemical build-up: low ozone levels are modeled

1 over the city of Paris (36-38 ppb) due to titration by NO (road transport mainly) and higher
2 levels (47-50 ppb) are modeled at the surrounding rural area due to photochemical formation.
3 Projections show an increase in maximum ozone (+7 ppb) over the city of Paris under the REF
4 scenario relative to CTL and only a small decrease under the MIT scenario (-3.5 ppb). The
5 average daytime ozone (not shown) also increases substantially in downtown Paris by
6 approximately +10 ppb under REF. The results are consistent with the near future projection of
7 Roustan et al. (2011) who also employed local scale emissions and modelled maximum ozone
8 increase in Paris for the year 2020. Reductions in rural ozone are modelled under both scenarios:
9 REF: -3.2 ppb and MIT: -13.5 ppb.

10 Previous studies have shown that anthropogenic emissions over urban areas are the driver of
11 ozone concentrations compared to climate, boundary conditions and other influencing factors
12 (Colette et al., 2013). Therefore, to gain further insight in the ozone response one should study
13 the differences between present and future time ozone precursors' emissions. However emission
14 changes under different chemical regimes may also lead to different ozone responses. For
15 example, air-quality projections conducted at a 0.5°x0.5° resolution grid over Europe forced with
16 GEA emissions and the same meteorology as in our study found significant decrease compared
17 to present time values in ozone concentrations over the Paris region at the 2050 horizon for both
18 REF (-5 ppb) and MIT (-16 ppb) scenarios (Colette et al., 2013), in contrast to our findings
19 showing increase in ozone under the REF scenario and only small decrease under the MIT
20 scenario. We are interested to see whether this difference in the sign between the local and
21 regional ozone projections could be explained by the photochemical regime under which ozone
22 is produced in each simulation.

23

24 **4.2.1 Analysis of the chemical regimes**

25 It is known that areas under NO_x-sensitivity or VOC-sensitivity are more effectively mitigated
26 when NO_x or NMVOCs emission reductions are implemented respectively (Beekman and
27 Vautard, 2010). Previous modeling exercises using the CHIMERE model have shown that the
28 ozone photochemistry in Paris is VOC-sensitive (Beekman and Derognat, 2003; Beekman and
29 Vautard, 2010; Deguillaume et al., 2008).

30 In this experiment we perform a model sensitivity analysis in which anthropogenic NO_x and
31 NMVOCs emissions let vary from a factor of one fourth up to two times their actual value with a

1 step of 0.25 (all combinations of 8 different scenarios for both NO_x and NMVOCs). In total 64
2 simulations were performed for a typical summertime ozone episode. Emission changes were
3 applied over the whole 3-dimensional domain. We conducted the same experiment twice: once
4 using as initial local-scale emission inventory developed by AIRPARIF (LOC case) and once
5 using the regional scale inventory (REG case). In order to isolate the effect of emissions only and
6 exclude the potential impact of other resolution-related effects the sensitivity analysis for the
7 REG realization was not performed in the native REG domain; instead we first downscaled the
8 regional emission inventory on the 4km grid and then ran the regional scale simulation.
9 Obviously, emission totals between the two simulations do not match and no direct comparison
10 should be made based on these results. However, it is interesting to see how different emission
11 starting points may lead to ozone production under different photochemical regimes and
12 therefore to different future ozone projections. We note that present time NO_x /NMVOCs
13 emission ratios within the ozone period over Paris are much higher in the LOC inventory than in
14 the REG dataset (0.5 vs. 0.2). This ratio is a key factor for the modeling of ozone production. We
15 chose to run the sensitivity analysis over a one-day, present time, summer ozone episode that
16 emission fluxes and meteorological conditions favoring the photochemical ozone built-up are
17 similar in most ozone events.

18 Iso-contours of day ozone maxima concentrations as a function of NO_x and NMVOCs emission
19 rates are given for the two simulations (isopleth plots of Fig. 5). Two cases are discussed
20 separately: downtown chemistry (panels a and b) and in-plume chemistry (panels c and d). “In-
21 plume” corresponds to the chemical reactions taking place when high concentrations of nitrous
22 oxides coming from the city and NMVOCs from the rural areas help to accumulate ozone on the
23 downwind site of the city. To extract “in-plume” results we identify at each hour of the simulated
24 episode the grid cell with the maximum concentrations inside the domain. Downtown chemistry
25 in the LOC simulation is mainly sensitive to NO_x changes with sharp ozone increases related to
26 NO_x reductions. This is a typical ozone response near high NO_x emission sources where titration
27 and removal of radicals by nitrogen dioxide are the main drivers of ozone concentrations (VOC-
28 sensitive regime). Under the REF scenario NO_x reductions in 2050 are much more drastic than
29 NMVOC ones (Table 1) because the GEA-derived scaling coefficients used to project local scale
30 emissions from 2020 to 2050 mainly implement NO_x reductions through domestic heating and
31 road transport regulation. Under VOC-sensitive conditions NO_x reductions without additional

1 regulation of NMVOCs lead to inhibited ozone titration and increase in ozone concentrations.
2 Ozone mitigation would most likely be more effective if the domestic/industrial use of solvents
3 (the main source of NMVOCs) were targeted as well. Under the MIT scenario however, where
4 both NO_x and NMVOCs are mitigated more effectively ozone concentrations decrease in 2050
5 compared to present time levels. Chemistry in the REG simulation on the other hand is driven by
6 a NO_x-sensitive regime. The titration process is much less pronounced compared to the LOC run.
7 As a result ozone decreases in response to the significant NO_x reductions (see also discussion in
8 Sect. 2.3) under both REF and MIT scenarios.

9 In the regional setup both urban and rural chemistry is characterized by NO_x-sensitive conditions
10 (panel b vs. d). On the contrary, if urban chemistry is clearly VOC-sensitive at the local scale run
11 (panel a), in-plume ozone built-up is found on the ridge line separating the two regimes (panel c).
12 This is consistent with previous studies (Menut et al., 2000; Sillman et al., 2003). Urban ozone
13 levels modeled at the local scale are much lower than those modeled at the regional scale by
14 almost 50 ppb (~54 ppb vs. ~100 ppb). This is due to the higher NO_x emission ratios prescribed
15 by the local scale inventory (LOC) compared to the regional inventory (REG). As far as the in-
16 plume chemistry is concerned the difference between the two simulations is less pronounced
17 (~20 ppb). This is consistent with the fact that the reductions in rural ozone modelled at regional
18 scale (REF: -3.2 ppb and MIT: -13.5 ppb) and in our study for the two future projections relative
19 to present time levels are similar. Photochemical ozone built-up occurs at longer time and space
20 scale compared to titration and therefore the increase in the resolution of the emissions brought
21 about at the local scale does not provide much new information to the modeling of rural ozone.

22 This sensitivity analysis shows that the integration of high-resolution emission projections in the
23 modeling of ozone is critical. Clearly the regional and local simulation will respond differently to
24 emission changes in the future but unfortunately it is not possible to assess quantitatively the
25 impact of this change since besides the spatial gradients in emissions, projections also differ
26 between the LOC and REG simulations. The conclusion that can be drawn though from this
27 sensitivity analysis is that the simulation forced by the regional scale emissions fails to
28 distinguish the chemical regime between urban and rural chemistry (both shown as NO_x-limited)
29 and that ozone titration over Paris is most likely underestimated in the regional setup which may
30 explain the ozone decrease modelled for 2050 over Paris under the REF scenario. Increase in

1 ozone due to sharp NO_x emission reductions under a VOC-limited environment as modelled with
2 the local setup may be more realistic.

3

4 **4.2.2 Future chemical regimes indicators**

5 Based on the aforementioned previous studies as well as on the sensitivity exercise carried out
6 here, ozone formation in the city of Paris occurs under VOC-sensitive conditions. However, it is
7 plausible that the implementation of emission reductions in the long run causes a shift of the
8 chemical regime towards a more NO_x -sensitive chemistry (Beekman and Vautard, 2010; Colette
9 et al., 2012; Tarasson et al., 2003).

10 To investigate this shift, we use here a number of chemical regime indicators, which explain
11 emission accumulation and radical production/loss processes: O_3/NO_y , O_3/NO_z and $\text{H}_2\text{O}_2/\text{NO}_z$.
12 Each indicator accounts for different aspects of ozone chemistry, for example the $\text{H}_2\text{O}_2/\text{NO}_z$ ratio
13 takes into account both the impact of emissions and radical production (Sillman, 1995) by
14 comparing the $\text{HO}_x + \text{NO}_x$ radical sink (yielding NO_z) to the $\text{HO}_2 + \text{HO}$ radical sink yielding
15 H_2O_2 . The latter sink corresponds to enhanced radical production, which favors NO_x -sensitive
16 conditions (Kleinman, 1997). These indicators are used in order to avoid the large number of
17 sensitivity runs such as the ones described in Sect. 4.2.1 that would be necessary to perform if
18 one used a more direct approach such as above.

19 Chemical regime indicators are estimated from domain-wide daytime O_3 , NO_y , NO_z and H_2O_2
20 concentrations for the CTL run and the two REF and MIT projections (Fig. 6). Higher O_3/NO_y ,
21 O_3/NO_z and $\text{H}_2\text{O}_2/\text{NO}_z$ ratios point to more NO_x -sensitive conditions while lower ratio values
22 point to VOC-sensitive chemistry. A visual inspection of the figure reveals that all three
23 chemical indicator ratios increase under both REF and MIT scenarios compared to CTL due to
24 decreases in NO_y and NO_z concentrations induced by the implemented NO_x emission reductions.
25 For example the decade mean O_3/NO_y molar ratio shifts from the preset-time value of 0.64 to
26 2.75 and 10.6 in the REF and MIT scenarios respectively. Based on these indicators we deduce
27 that a shift towards more NO_x -sensitive chemistry should be expected in 2050 under both REF
28 and MIT scenarios.

29

30 **4.2.3 Ozone health indicators**

1 Here, we study how different ozone health indicators change under the two future scenarios
2 (Table 4). We focus on three indexes: i) the sum of the differences between maximum daily 8-
3 hour running means and the 35 ppb threshold value (SOMO35); ii) the number of days where
4 maximum daily 8-hour running mean ozone concentration exceeds the 60 ppb threshold (Nd120)
5 and iii) the mean of the ten highest daily max concentrations during the ozone period (MTDM).
6 These metrics are typically used in health impact assessment studies and account for the non-
7 linearity in the ozone dose-response function. For example SOMO35 was developed in the Joint
8 WHO/Convention Task Force in 2004 and represents the cumulative annual exposure to ozone.
9 The threshold value was established on the fact that a statistically significant increase in
10 mortality risk estimates was observed at ozone concentrations above 25–35ppb. .
11 Under the REF scenario SOMO35 modelled at local scale in the city is almost doubled compared
12 to present-time (Table 4) while the reductions of the Nd120 index from 29 to 18 days points to
13 less frequent ozone episodes in the future. The MTDM index remains constant suggesting that
14 ozone episodes will not decrease in intensity.
15 All three health related proxies improve under the MIT scenario. SOMO35 decreases by 79%
16 and MTDM by 26.5% relative to CTL corresponding to future conditions with no significant
17 ozone episodes (Nd120 falls to zero). The modelled reductions in the health indicators represent
18 a much more efficient mitigation compared to maximum ozone concentrations (see discussion in
19 Sect. 4.2) highlighting the high sensitivity of these indicators to their respective cut-off
20 thresholds. It becomes clear, that from a human health perspective the MIT scenario is very
21 effective and the co-benefits of climate and air quality strategies are significant. In the downwind
22 rural areas south of Paris all health indicators under both scenarios are improved, as seen in
23 Table 4, following the subsiding of ozone levels in the future (Fig. 4).

24

25 **4.3 PM_{2.5}**

26 Local scale PM_{2.5} projections (wintertime) are presented in Fig. 7 as well as differences between
27 each of the REF and MIT scenarios and the CTL simulation. Major decrease in PM_{2.5} is
28 modelled under both REF and MIT projections compared to present time levels. This is mainly
29 due to significant reductions in primary particle emissions (Table 1). In downtown Paris,
30 concentrations are reduced from 14.2 µg/m³ in CTL to 3.4 µg/m³ and 1.6 µg/m³ under the REF
31 and MIT scenarios respectively. The reductions are much stronger in the city than at rural areas

1 due to the effective mitigation of road transport emissions. Consequently the large wintertime
2 urban increment (difference between urban and rural concentrations) of approximately $6.8 \mu\text{g}/\text{m}^3$
3 modelled with CTL is significantly reduced in both future projections: $\sim 1 \mu\text{g}/\text{m}^3$ in REF and less
4 than $0.2 \mu\text{g}/\text{m}^3$ in MIT.

6 **5 Conclusions**

7 Mid-21st century ozone and $\text{PM}_{2.5}$ projections over the city of Paris have been modelled with the
8 CHIMERE air-quality model at a 4 km horizontal resolution under two consistent climate and
9 emission scenarios: a reference and a mitigation scenario. To our knowledge, this is the first time
10 that a study of a 10-year air-quality projection under climate and city level emission changes is
11 conducted over a large European agglomeration at such fine scale. A key innovation of this work
12 is that we use local-scale emissions and their projections until 2020 developed by local experts
13 (AIRPARIF) and extend those until 2050 based on coefficients extracted from large-scale
14 emission projections. A 10-year control simulation served model evaluation purposes.
15 Furthermore, we investigate how ozone projections under the two future scenarios depend on the
16 photochemical regime.

17 Model evaluation showed a very good agreement between model and measurements for ozone
18 and an underestimation of wintertime $\text{PM}_{2.5}$ by 20% over the urban area, which is mainly
19 attributed to a large wet bias in wintertime precipitation (+26.5%). The comparison between
20 modeled and measured O_x showed that the model at 4 km resolution accurately resolves O_3
21 titration by NO over the highly urbanized city of Paris. The decade average bias within the ozone
22 period for O_x ($\text{O}_3 + \text{NO}_2$) and ozone is found to be less than 0.3 ppb.

23 Under the reference scenario ozone increases over the city of Paris by +7 ppb relative to present
24 time values and only a small decrease is modelled under the mitigation scenario (-3.5 ppb).
25 Through a sensitivity analysis, we showed that ozone formation in Paris occurs under VOC-
26 sensitive chemistry. Under such conditions and due to the stronger mitigation of NO_x compared
27 to NMVOCs in the REF scenario, titration is inhibited and ozone increases in the 2050 horizon.
28 Following the MIT trajectory both NO_x and NMVOCs are more effectively regulated leading to
29 ozone reduction in 2050. The same sensitivity analysis applied on the regional emission
30 projections showed that ozone formation in Paris occurred under NO_x -sensitive conditions. The
31 discrepancy in the chemical regime is attributed to differences in ozone precursor emissions

1 prescribed by the two inventories: NO_x/NMVOCs emission ratios are much lower in the regional
2 (0.2) compared to the local inventory (0.5). Modelling at regional scale most likely
3 underestimates ozone titration prescribing NO_x-limited chemistry for Paris. Under this chemical
4 regime ozone precursor emission cutbacks prescribed even for the less optimistic REF scenario
5 benefits ozone air quality to such an extent that reductions are observed while the local setup
6 yields ozone increases instead. If the regional scale model is inadequate to resolve urban features
7 of ozone chemistry, mainly titration close to high NO_x emission sources, it yields similar rural
8 ozone levels as the local scale run showing that the longer time-scale processes of emission
9 transport and ozone formation are less sensitive to model resolution in the high ozone
10 concentration plume. Our findings suggest that the estimates based on European scale
11 applications are likely to overestimate the downward ozone trend under VOC-sensitive
12 conditions while differences in rural areas are limited.

13 Finally in downtown Paris, PM_{2.5} concentrations are reduced by 78% and 89% under the REF
14 and MIT scenarios respectively. The reduction is much more prominent over the urban part of
15 the domain due to significant reductions in primary emissions as a result of the effective
16 mitigation of the road transport and residential sectors. Therefore the large urban increment
17 modelled at the control run is significantly reduced in both future projections.

18

19 **Acknowledgements**

20 The project is funded by the GIS-Climat, the French Environment and Energy Management
21 Agency Ademe, contract n° 1110C0073.

22

23

24

25

26

27

28

29

30

31

1 **References**

- 2 AIRPARIF, Evaluation Prospective des emissions et des concentrations des polluants atmospheriques a
3 l'horizon 2020 en Ile-De-France – Gain sur les emissions en 2015. Report available at
4 http://www.airparif.asso.fr/_pdf/publications/ppa-rapport-121119.pdf, 2012.
- 5 Amann, M., Bertok, I., Borken-Kleefeld, J., Cofala, J., Heyes, C., Höglund-Isaksson, L., Klimont, Z.,
6 Nguyen, B., Posch, M., Rafaj, P., Sandler, R., Schöpp, W., Wagner, F. and Winiwarter, W. Cost-effective
7 control of air quality and greenhouse gases in Europe: Modeling and policy applications, *Environ. Model.*
8 *Software*, 26, 1489-1501, 2011.
- 9 Arunachalam, S., Holland, A., Do, B. and Abraczinskas, M. A quantitative assessment of the influence of
10 grid resolution on predictions of future-year air quality in North Carolina, USA, *Atmos. Environ.*, 40,
11 5010–5026, 2006.
- 12 Beekmann, M. and Derognat, C. Monte Carlo uncertainty analysis of a regional-scale transport chemistry
13 model constrained by measurements from the Atmospheric Pollution Over the Paris Area (ESQUIF)
14 campaign, *J. Geophys. Res.*, 108(D17), 8559, doi:10.1029/2003JD003391, 2003.
- 15 Beekmann, M. and Vautard, R. A modelling study of photochemical regimes over Europe: robustness and
16 variability, *Atmos. Chem. Phys.*, 10, 10067-10084, 2010.
- 17 Bessagnet B., Seigneur, C. and Menut, L. Impact of dry deposition of semi-volatile organic compounds
18 on secondary organic aerosols, *Atmos. Environ.*, 44, 1781-1787, 2010.
- 19 Brasseur, G.P., et al., Past and future changes in global tropospheric ozone: impact and radiative forcing,
20 *Geophys. Res. Lett.*, 25, 3807-3810, 1998.
- 21 Butler, T.M., Stock, Z.S., Russo, M.R. Denier van der Gon, H.A.C. and Lawrence, M.G. Megacity ozone
22 air quality under four alternative future scenarios, *Atmos. Chem. Phys.*, 12, 4413–4428, 2012.
- 23 Chen, F. and Dudhia, J. Coupling an advanced land-surface/hydrology model with the Penn State/ NCAR
24 MM5 modeling system. Part I: model description and implementation, *Mon. Weather Rev.*, 129, 569–
25 585, 2001.
- 26 Cohan, D.S., Hu, Y. and Russell, A.G.: Dependence of ozone sensitivity analysis on grid resolution,
27 *Atmos. Environ.*, 40, 126–135, 2006.
- 28 Colette, A., Granier, C., Hodnebrog, O., Jakobs, H., Maurizi, A., Nyiri, A., Rao, S., Amann, M.,
29 Bessagnet, B., D'Angiola, A., Gauss, M., Heyes, C., Klimont, Z. and Meleux, F. Future air quality in
30 Europe: a multi-model assessment of projected exposure to ozone, *Atmos. Chem. Phys.*, 12, 10613-
31 10630, 2012.
- 32 Colette, A., Bessagnet, B., Vautard, R., Szopa, S., Rao, S., Schucht, S., Klimont, Z., Menut, L., Clain, G.,
33 Meleux, F. and Rouil, L. European atmosphere in 2050, a regional air quality and climate perspective
34 under CMIP5 scenarios, *Atmos. Chem. Phys.*, 13, 7451–7471, 2013.

1 Deguillaume, L., Beekmann, M. and Derognat, C.: Uncertainty evaluation of ozone production and its
2 sensitivity to emission changes over the Ile-de-France region during summer periods, *J. Geophys. Res.*,
3 113, D02304, doi:10.1029/2007JD009081, 2008.

4 Deser, C., Phillips, A., Bourdette, V. and Teng, H. Y. Uncertainty in climate change projections: the role
5 of internal variability. *Clim. Dynam.*, 38, 527-546, 2012.

6 Dudhia, J. Numerical study of convection observed during the winter monsoon experiment using a
7 mesoscale two-dimensional model, *J. Atmos. Sci.*, 46, 3077–3107, 1989.

8 Dufresne, J.-L., et al. Climate change projections using the IPSL-CM5 Earth System Model: from CMIP3
9 to CMIP5. *Clim. Dynam.*, 40, 2123-2165, 2013.

10 EPA, Guidance on the Use of Models and Other Analyses for Demonstrating Attainment of Air Quality
11 Goals for Ozone, PM2.5 and Regional Haze. EPA -454/B-07-002, April, 2007.

12 Fiore, A.M., Naik, V., Spracklen, D.V., Steiner, A., Unger, N., Prather, M., Bergmann, D., Cameron-
13 Smith, P.J., Cionni, I., Collins, W.J., Dalsøren, S., Eyring, V., Folberth, G.A., Ginoux, P., Horowitz,
14 L.W., Josse, B., Lamarque, J.-F., MacKenzie, I.A., Nagashima, T., O’Connor, F.O., Righi, M., Rumbold,
15 S.T., Shindell, D.T., Skeie, R.B., Sudo, K., Szopa, S., Takemura, T. and Zeng, G. Global air quality and
16 climate, *Chem. Soc. Rev.*, 41, 6663-6683, 2012.

17 Forkel, R. and Knoche, R. Regional climate change and its impact on photooxidant concentrations in
18 southern Germany: Simulations with a coupled regional climate–chemistry model, *J. Geophys. Res.*, 111,
19 D12302, doi:10.1029/2005JD006748, 2006.

20 Forkel, R. and Knoche, R. Nested regional climate–chemistry simulations for central Europe, *CR Geosci.*,
21 339, 734-746, 2007.

22 GEA: Global Energy Assessment - Toward a Sustainable Future, Chapter 17: Energy Pathways for
23 Sustainable Development, Cambridge University Press, Cambridge, UK and New York, NY, USA and
24 the International Institute for Applied Systems Analysis, Laxenburg, Austria. Available at
25 <http://www.iiasa.ac.at/web/home/research/Flagship-Projects/Global-Energy-Assessment/Home>
26 [GEA.en.html](http://www.iiasa.ac.at/web/home/research/Flagship-Projects/Global-Energy-Assessment/Home), 2012.

27 Granier, C., Bessagnet, B., Bond, T., D’Angiola, A., Denier Van Der Gon, H., Frost, G., Heil, A., Kaiser,
28 J., Kinne, S., Klimont, Z., Kloster, S., Lamarque, J.-F., Liousse, C., Masui, T., Meleux, F., Mieville, A.,
29 Ohara, T., Raut, J.-C., Riahi, K., Schultz, M., Smith, S., Thompson, A., Van Aardenne, J., Van Der Werf,
30 G. and Van Vuuren, D. Evolution of anthropogenic and biomass burning emissions of air pollutants at
31 global and regional scales during the 1980–2010 period, *Clim. Change* 109, 163–190, 2011.

32 Guenther, A., Karl, T., Harley, P., Wiedinmyer, C., Palmer, P. I. and Geron, C. Estimates of global
33 terrestrial isoprene emissions using MEGAN (Model of Emissions of Gases and Aerosols from Nature),
34 *Atmos. Chem. Phys.*, 6, 3181–3210, doi:10.5194/acp-6-3181-2006, 2006.

1 Hauglustaine, D. A., Hourdin, F., Jourdain, L., Filiberti, M.-A., Walters, S, Lamarque, J.F. and Holland,
2 E.A. Interactive chemistry in the Laboratoire de Meteorologie Dynamique general circulation model:
3 Description and background tropospheric chemistry evaluation, *J. Geophys. Res.*, 190, D04314,
4 doi:10.1029/2003JD003957, 2004.

5 Hauglustaine, D.A., Schulz, M., Balkanski, Y. and Cozic, A. A global model simulation of present and
6 future nitrate aerosols and their direct radiative forcing of climate, in preparation, 2013.

7 Hodzic, A., Vautard, R., Bessagnet, B., Lattuati, M., and Moreto, F. On the quality of long-term urban
8 particulate matter simulation with the CHIMERE model. *Atmos. Environ.*, 39, 5851-5864. 2005.

9 Hodzic, A., Jimenez, J.L., Madronich, S., Canagaratna, M.R., DeCarlo, P.F., Kleinman, L. and Fast, J.
10 Modeling organic aerosols in a megacity: potential contribution of semi-volatile and intermediate
11 volatility primary organic compounds to secondary organic aerosol formation, *Atmos. Chem. Phys.*, 10,
12 5491-5514

13 Hogrefe, C., Lynn, B., Civerolo, K., Ku, J.-Y., Rosenthal, J., Rosenzweig, C., Goldberg, R., Gaffin, S.,
14 Knowlton, K. and Kinney, P.L. Simulating changes in regional air pollution over the eastern United
15 States due to changes in global and regional climate and emissions. *J. Geophys. Res.*, 109, D22301,
16 doi:10.1029/2004JD004690, 2004.

17 Hong, S.-Y. and Lim, J.-O. The WRF Single-Moment 6-Class Microphysics Scheme (WSM6), *J. Korean*
18 *Meteor. Soc.*, 42, 129–151, 2006.

19 Intergovernmental Panel on Climate Change, *Climate change 2001: the Scientific Basis. Contribution of*
20 *Working Group I to the Third Assessment Report of the IPCC*, Cambridge University Press, Cambridge,
21 UK, and New York, USA. Available at <http://www.ipcc.ch>, 2001.

22 Intergovernmental Panel on Climate Change (IPCC), *Climate change 2007: the Physical Science Basis.*
23 *Contribution of Working Group I to the Fourth Assessment Report of the IPCC.* Available at
24 <http://www.ipcc.ch>, 2007.

25 Jacob, D.J. and Winner, D.A. Effect of climate change on air quality, *Atmos. Environ.*, 43, 51-63, 2009.

26 Jimenez, P.A. and Dudhia, J. Improving the Representation of Resolved and Unresolved Topographic
27 Effects on Surface Wind in the WRF Model. *J. Applied Meteorol. Climatol.*, 51, 300-316, 2012.

28 Kain, J.S. The Kain–Fritsch Convective Parameterization: An Update, *J. Appl. Meteor.*, 43, 170–181,
29 2004.

30 Kelly, J., Makar, P.A. and Plummer, D.A. Projections of mid-century summer air-quality for North
31 America: effects of changes in climate and precursor emissions, *Atmos. Chem. Phys.*, 12, 5367-5390,
32 2012.

1 Kleinman, L.I., Daum, P.H., Lee, J.H., Lee, Y.-N., Nunnermacker, L.J., Springston, S.R., Newman, L.,
2 Weinstein-Lloyd, J. and Sillman, S. Dependence of ozone production on NO and hydro-carbons in the
3 troposphere, *Geophys. Res. Lett.*, 24, 2299–2302, 1997.

4 Knowlton, K., Rosenthal, J.E., Hogrefe, C., Lynn, B., Gaffin, S., Goldberg, R., Rosenzweig, C., Civerolo,
5 K., Ku, J.-Y. and Kinney, P.L. Assessing Ozone-Related Health Impacts under a Changing Climate,
6 *Environ. Health Perspect.*, 112 (15), 1557-1563, 2004.

7 Lam, Y.F., Fu, J.S., Wu, S. and Mickley, L.J. Impacts of future climate change and effects of biogenic
8 emissions on surface ozone and particulate matter concentrations in the United States, *Atmos. Chem.*
9 *Phys.*, 11, 4789–4806, 2011.

10 Lamarque, J.-F., Bond, T. C., Eyring, V., Granier, C., Heil, A., Klimont, Z., Lee, D., Liousse, C.,
11 Mieville, A., Owen, B., Schultz, M.G., Shindell, D., Smith, S.J., Stehfest, E., Van Aar-den-nee, J., Cooper,
12 O.R., Kainuma, M., Mahowald, N., Mc-Connell, J.R., Naik, V., Riahi, K., and van Vuuren, D.P.
13 Historical (1850–2000) gridded anthropogenic and biomass burning emissions of reactive gases and
14 aerosols: methodology and application, *Atmos. Chem. Phys.*, 10, 7017-7039, doi:10.5194/acp-10-7017-
15 2010, 2010.

16 Langner, J., Bergstrom, R. and Foltescu, V. Impact of climate change on surface ozone and deposition of
17 sulphur and nitrogen in Europe, *Atmos. Environ.*, 39, 1129–1141, 2005.

18 Langner, J., Engardt, M., Baklanov, A., Christensen, J. H., Gauss, M., Geels, C., Hedegaard, G. B.,
19 Nuterman, R., Simpson, D., Soares, J., Sofiev, M., Wind, P. and Zakey, A. A multi-model study of
20 impacts of climate change on surface ozone in Europe. *Atmos. Chem. Phys.* 12, 10423-10440, 2012.

21 Lattuati, M.: Contribution a l'étude du bilan de l'ozone tropospherique a l'interface de l'Europe et de
22 l'Atlantique Nord: modelisation lagrangienne et mesures en altitude, Phd thesis, Universite P.M.Curie,
23 Paris, France, 1997.

24 Liao, H., Chen, W.-T. and Seinfeld, J.H. Role of climate change in global predictions of future
25 tropospheric ozone and aerosols, *J. Geophys. Res.* 111, doi:10.1029/2005JD006862, 2006.

26 Markakis, K., Poupkou, A., Melas, D. and Zerefos, C. A GIS based methodology for the compilation of
27 an anthropogenic PM₁₀ emission inventory in Greece, *Atmos. Poll. Res.*, 1 (2), 71-81, 2010.

28 Markakis, K., Im, U., Unal, A., Melas, D., Yenigün, O. and İncecik, S. Compilation of a GIS based high
29 spatially and temporally resolved emission inventory for the İstanbul Greater Area, *Atmos. Poll. Res.*, 3,
30 112-125, 2012.

31

32 Menut, L., Coll, I. and Cautenet, S., Impact of meteorological data resolution on the forecasted ozone
33 concentrations during the ESCOMPTE IOP2a and IOP2b, *Atmos. Res.*, 74, 139–159, 2005a.

1 Menut, L., Schmechtig, C. and Marticorena, V. Sensitivity of the sandblasting fluxes calculations to the
2 soil size distribution accuracy, *J. Atmos. Ocean. Technol.*, 22, 1875–1884, 2005b.

3 Menut, L., Bessagnet, B., Khvorostiyarov, D., Beekmann, M., Colette, A., Coll, I., Gurci, G., Foret, G.,
4 Mailler, S., Monge, J.-L., Turquety, S., Valari, M., Vautard, R. and Vivanco, M.G. Regional atmospheric
5 composition modeling with CHIMERE. *Geosci. Model Dev.* 6, 203-329, 2013.

6 Mlawer, E.J., Taubman, S.J., Brown, P.D., Iacono, M.J. and Clough, S.A. Radiative transfer for
7 inhomogeneous atmospheres: RRTM, a validated correlated-k model for the longwave. *J. Geophys. Res.*,
8 102, 16663–16682, 1997.

9 Nenes, A., Pilinis, C. and Pandis, S. ISORROPIA: A new thermodynamic model for inorganic
10 multicomponent atmospheric aerosols, *Aquatic Geochem.*, 4, 123–152, 1998.

11 Nolte, C.G., Gilliland, A.B., Hogrefe, C. and Mickley, L.J. Linking global to regional models to assess
12 future climate impacts on surface ozone levels in the United States, *J. Geophys. Res.*, 113, D14307,
13 doi:10.1029/2007JD008497, 2008.

14 Pleim, J.E. A combined local and nonlocal closure model for the atmospheric boundary layer. Part I:
15 Model description and testing, *J. Appl. Meteorol. Climatol.*, 46, 1383–1395, 2007.

16 Prather, M., et al. Fresh air in the 21st century? *Geophys. Res. Lett.*, 30 (2), 1100,
17 doi:10.1029/2002GL016285, 2003.

18 Rao, S., Chirkov, V., Dentener, F., Van Dingenen, R., Pachauri, S., Purohit, P., Amann, M., Heyes, C.,
19 Kinney, K., Kolp, P., Klimont, Z., Riahi, K. and Schoepf, W. Environmental Modeling and Methods for
20 Estimation of the Global Health Impacts of Air Pollution, *Environ. Model. Assess.*, 17, 613–622, 2012.

21 Rao, S., Pachauri, S., Dentener, F., Kinney, P., Klimont, Z., Riahi, K. and Schöpp, W. Better air for better
22 health: Forging synergies in policies for energy access, climate change and air pollution, *Global Environ.*
23 *Chang.*, doi: 10.1016/j.gloenvcha.2013.05.003, 2013.

24 Riahi, K., Gruebler, A. and Nakicenovic, N., Scenarios of long-term socio-economic and environmental
25 development under climate stabilization, *Technol. Forecast. Soc. Change* 74, 2007.

26 Riahi, K., Rao, S., Krey, V., Cho, C., Chirkov, V., Fischer, G., Kindermann, G., Nakicenovic, N. and
27 Rafaj, P. RCP 8.5-A scenario of comparatively high greenhouse gas emissions, *Clim. Change*, 109, 33–
28 57, 2011.

29 Riahi, K., Dentener, F., Gielen, D., Grubler, A., Jewell, J., Klimont, Z., Krey, V., McCollum, D.,
30 Pachauri, S., Rao, S., van Ruijven, B., van Vuuren, D.P. and Wilson, C. Energy Pathways for Sustainable
31 Development, in: Nakicenovic, N. (Ed.), *Global Energy Assessment: Toward a Sustainable Future*.
32 IIASA, Laxenburg, Austria and Cambridge University Press, Cambridge, United Kingdom and New
33 York, NY, 2012.

1 Roustan, Y., Pausader, M. and Seigneur, C. Estimating the effect of on-road vehicle emission control on
2 future air quality in Paris, France, *Atmos. Environ.*, 45, 6828-6836, 2011.

3 Schaap, M., Manders, A.M.M., Hendriks, E.C.J., Cnossen, J.M., Segers, A.J.S., Denier van der Gon,
4 H.A.C., Jozwicka, M., Sauter, F.J., Velders, G.J.M., Matthijsen J. and Builtjes P.J.H. Regional modelling
5 of particulate matter for the Netherlands. Available at www.pbl.nl, 2009.

6 Scire, J.S., Strimaitis, D.G. and Yamartino, R.J. Model formulation and user's guide for the CALPUFF
7 dispersion model. Sigma Research Corp., Concord, MA, 1990.

8 Sillman, S., Logan, J.A. and Wofsy, S.C. A regional scale model for ozone in the United States with
9 subgrid representation of urban and power plant plumes, *J. Geophys. Res.* 95, 5731–5748, 1990.

10 Sillman, S. The use of NO_y, H₂O₂, and HNO₃ as indicators for ozone-NO_x-hydrocarbon sensitivity in
11 urban locations, *J. Geophys. Res.*, 100(D7), 14,175–14,188, 1995.

12 Sillman, S. and Samson, F.L. Impact of temperature on oxidant photochemistry in urban, polluted rural
13 and remote environments, *J. Geophys. Res.*, 100 (D6), 11,497–11, 508, 1995.

14 Sillman, S., Vautard, R., Menut, L. and Kley, D. O₃-NO_x-VOC sensitivity and NO_x-VOC indicators in
15 Paris: Results from models and Atmospheric Pollution over the Paris Area (ESQUIF) measurements. *J.*
16 *Geophys. Res.*, 108, 8563, doi:10.1029/2002JD001561, 2003.

17 Skamarock, W.C. and Klemp J.B. A time-split non-hydrostatic atmospheric model, *J. Comput. Phys.*,
18 227, 3465–3485, 2008.

19 Simpson, D.W., Yttri, K., Klimont, Z., Caseiro, A., Gelencser, A., Pio, C., Puxbaum, H. and Legrand,
20 M.R. Modelling carbonaceous aerosol over Europe: analysis of the CARBOSOL and EMEP EC/OC
21 campaigns, *J. Geophys. Res.*, 112, D23S19. doi:10.1029/2006JD008158, 2007.

22 Solazzo, E., Bianconi, R., Pirovano, G., Volker, M., Vautard, R., Appel, K.W., Bessagnet, B., Brandt, J.,
23 Christensen, J.H., Chemel, C., Coll, I., Ferreira, J., Forkel, R., Francis, X.V., Grell, G., Grossi, P.,
24 Hansen, A., Miranda, A.I., Moran, M.D., Nopmongcol, U., Parnk, M., Sartelet, K.N., Schaap, M., Silver,
25 J.D., Sokhi, R.S., Vira, J., Werhahn, J., Wolke, R., Yarwood, G., Zhang, J., Rao, S.T. and S. Galmarini.
26 Operational model evaluation for particulate matter in Europe and North America in the context of the
27 AQMEII project, *Atmos. Environ.*, doi:10.1016/j.atmosenv.2012.02.045, 2011.

28 Solazzo, E., et al. Model evaluation and ensemble modeling for surface-level ozone in Europe and North
29 America, *Atmos. Environ.*, doi:10.1016/j.atmosenv.2012.01.003, 2012.

30 Stern, R., Builtjes, P., Schaap, M., Timmermans, R., Vautard, R., Hodzic, A., Memmesheimer, M.,
31 Feldmann, H., Renner, E., Wolke, R. and A. Kerschbaumer. A model inter-comparison study focusing on
32 episodes with elevated PM₁₀ concentrations, *Atmos. Environ.*, 42, 4567-4588, 2008.

33 Szopa, S., Hauglustaine, D.A., Vautard, R. and Menut, L. Future global tropospheric ozone changes and
34 impact on European air quality, *Geophys. Res. Lett.*, 33, L14805, doi:10.1029/2006GL025860, 2006.

1 Szopa, S. and Hauglustaine, D. Relative impacts of worldwide tropospheric ozone changes and regional
2 emission modifications on European surface-ozone levels, *CR Geosci.*, 339, 709-720, 2007.

3 Szopa, S., Balkanski, Y., Schulz, M., Bekki, S., Cugnet, D., Fortems-Cheiney, A., Turquety, S., Cozic, A.,
4 Deandreis, C., Hauglustaine, D., Idelkadi, A., Lathiere, J., Lefevre, F., Marchand, M., Vuolo, R., Yan, N.
5 and Dufresne, J.-L. Aerosol and ozone changes as forcing for climate evolution between 1850 and 2100,
6 *Clim. Dynam.*, 40, 2223-2250. 2013.

7 Tagaris, E., Liao, K.-J., DeLucia, A.J., Deck, L., Amar, P. and Russell, A.G. Potential impact of climate
8 change on air pollution-related human health effects, *Environ. Sci. Technol.*, 43, 4979-4988, 2009.

9 Tarasson, L., Jonson, J.E., Fagerli, H., Benedictow, A., Wind, P., Simpson, D. and Klein, H.
10 Transboundary acidification and eutrophication and ground level ozone in Europe: Source-Receptor
11 relationships, *Norw. Meteorol. Inst, Oslo*, 2003.

12 Tie, X., Brasseur, G. and Ying, Z. Impact of model resolution on chemical ozone formation in Mexico
13 City: application of the WRF-Chem model, *Atmos. Chem. Phys.*, 10, 8983–8995, 2010.

14 UNFPA: State of World Population 2007: Unleashing the Potential of Urban Growth, 2007.

15 Valari, M. and Menut, L. Does an Increase in Air Quality Models' Resolution Bring Surface Ozone
16 Concentrations Closer to Reality?, *J. Atmos. Ocean. Technol.*, 25, 1955-1968, 2008.

17 Valin, L.C., Russell, A.R., Hudman, R.C. and Cohen, R.C. Effects of model resolution on the
18 interpretation of satellite NO₂ observations, *Atmos. Chem. Phys.*, 11, 11647-11655, 2011.

19 Vautard R., Builtjes, P.H.J., Thunis, P., Cuvelier, C., Bedogni, M., Bessagnet, B., Honore, C.,
20 Moussiopoulos, N., Pirovano, G., Schaap, M., Stern, R., Tarasson, L. and Wind P. Evaluation and
21 intercomparison of Ozone and PM10 simulations by several chemistry transport models over four
22 European cities within the CityDelta project, *Atmos. Environ.*, 41 (1), 173-188, 2007.

23 Vautard, R., Bessagnet, B., Chin, M. and Menut, L. On the contribution of natural Aeolian sources to
24 particulate matter concentrations in Europe: testing hypotheses with a modelling approach, *Atmos.*
25 *Environ.*, 39, 3291–3303, 2005.

26 Vautard, R., Moran, M. D., Solazzo, E., Gilliam, R. C., Matthias, V., Bianconi, R., Chemel, C., Ferreira,
27 J., Geyer, B., Hansen, A. B., Jericevic, A., Prank, M., Segers, A., Silver, J. D., Werhahn, J., Wolke, R.,
28 Rao, S. T., and S. Galmarini. Evaluation of the meteorological forcing used for the Air Quality Model
29 Evaluation International Initiative (AQMEII) air quality simulations, *Atmos. Environ.*,
30 doi:10.1016/j.atmosenv.2011.10.065, 2012.

31 van Aardenne, J.A., Dentener, F.J., Olivier, J.G.J., Goldewijk, C.G.M.K. and Lelieveld, J. A 1 degrees x 1
32 degrees resolution data set of historical anthropogenic trace gas emissions for the period 1890-1990.
33 *Global Biogeochem. Cy*, 15 (4), 909-928, 2001.

1 van Vuuren, D., Edmonds, J., Kainuma, M., Riahi, K., Thomson, A., Hibbard, K., Hurtt, G., Kram, T.,
2 Krey, V., Lamarque, J.F., Ma-sui, T., Meinshausen, M., Nakicenovic, N., Smith, S., and Rose, S. The
3 representative concentration pathways: an overview, *Clim. Change*, 109, 5–31, 2011.

1 Table 1. Current time and future emission estimates (kt) over a 50km² area around Paris
2 extracted from the 1st model layer.

	NO _x ^a	NMVOCS ^a	PM _{2.5} ^b
CTL	11.2	22.6	1.5
2050 REF	3.1	10.6	0.34
2050 MIT	1.0	8.1	0.18

3 a ozone period (April-August)

4 b winter period

5

6

7

8

9

10

11

12

13

14

15

16

17

18

19

20

21

22

23

24

25

26

1 Table 2. Observed and modelled meteorological variables over the Ile-de-France region.
 2 Modelled data stem from the WRF simulation at 10km resolution. Absolute model bias is given
 3 in parenthesis.

Variable	Summer (JJA)		Winter (DJF)	
	Obs	Model	Obs	Model
7 stations average				
T2 (°C)	19.2	19.8 (+0.6)	4.3	4.2 (-0.1)
WS10 (m/s)	2.9	3.7 (+0.8)	3.6	5.5 (+1.9)
RH (%)	69.1	55.8 (-13.3)	85.0	83.9 (-1.1)
PRECIP (mm/day)	0.076	0.073 (-0.003)	0.07	0.094 (+0.024)
MONT (Paris)				
T2 (°C)	20.1	20.9 (+0.8)	5.4	4.9 (-0.5)
WS10 (m/s)	2.8	3.3 (+0.5)	3.3	4.7 (+1.4)
RH (%)	64.9	50.8 (-14.1)	79.8	79.5 (-0.3)
PRECIP (mm/day)	0.073	0.085 (+0.012)	0.064	0.081 (+0.017)

4
 5
 6
 7
 8
 9
 10
 11
 12
 13
 14
 15
 16
 17

1 Table 3. Future changes in key meteorological variables^a under the two simulated climate
 2 scenarios.

Variable	CTL	$\Delta(\text{REF-CTL})$	$\Delta(\text{MIT-CTL})$
Temperature ($^{\circ}\text{C}$)	11.6	+1.1	-0.5
RH (%)	72.3	+1.1	+1.7
Precipitation (mm/day)	0.1	+0.007	+0.22
Radiation (W/m^2)	154.3	-5.4	-25.4

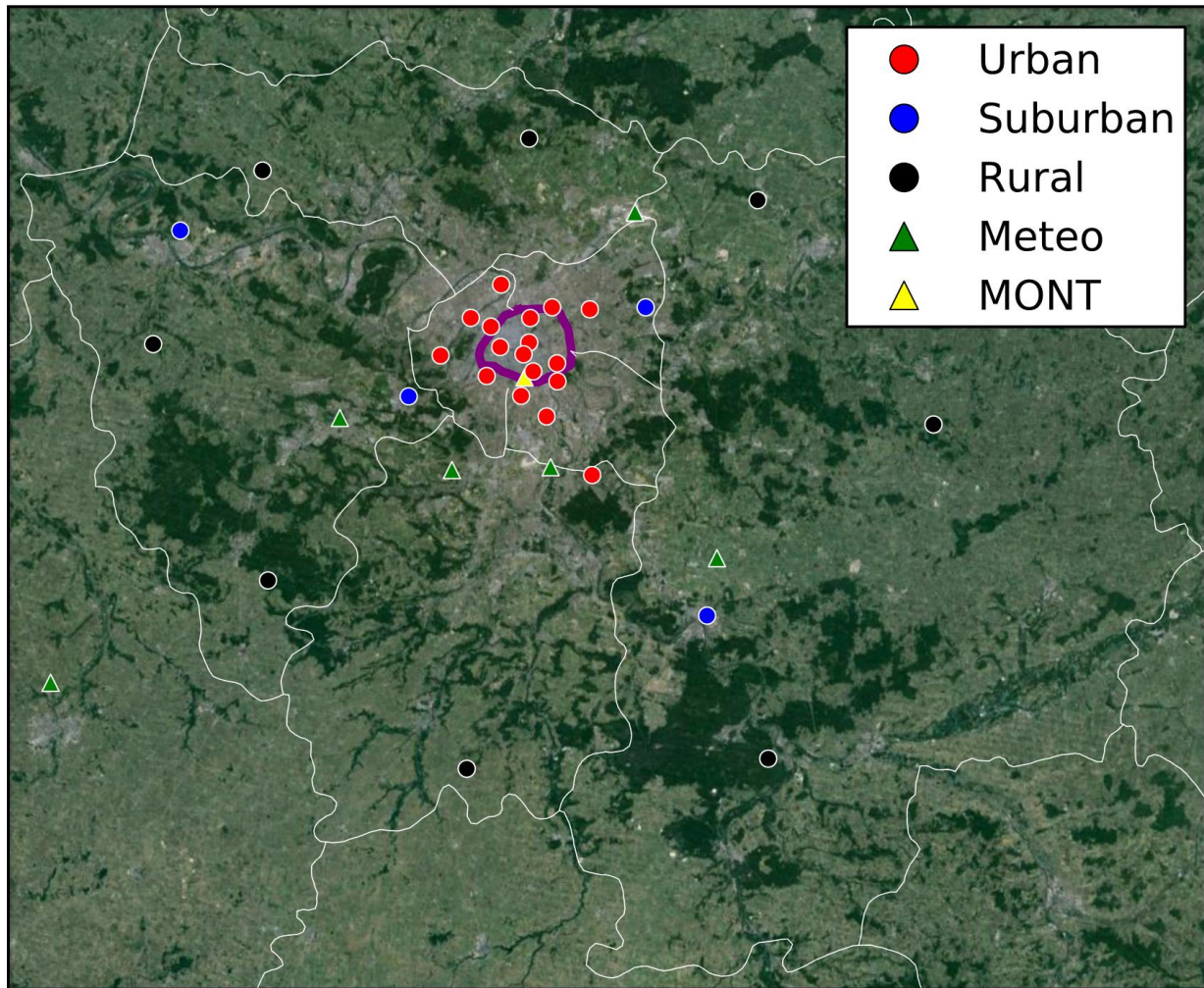
3 a Annual domain-wide values extracted from 10-yr mean of daily averages.

4
 5
 6
 7
 8
 9
 10
 11
 12
 13
 14
 15
 16
 17
 18
 19
 20
 21
 22
 23
 24
 25

1 Table 4. Ozone exposure indicators for the control simulation and the relative differences
 2 between the latter and the two future projections for the city of Paris.

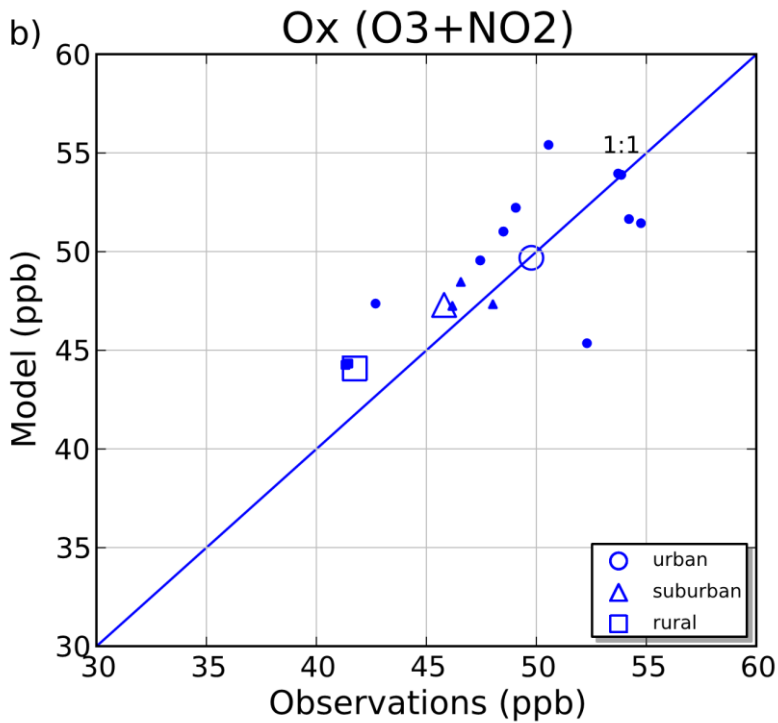
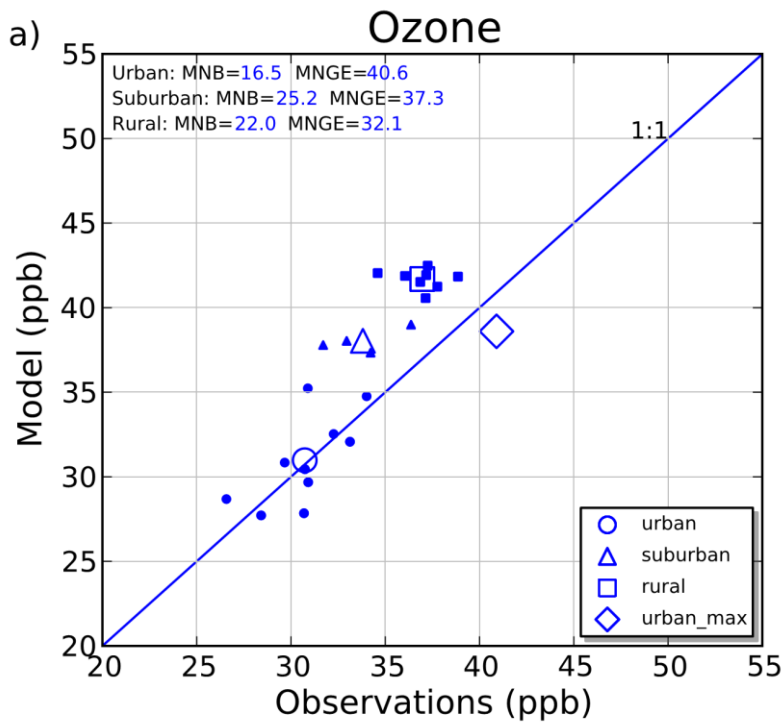
Variable	CTL	REF	MIT
City			
SOMO35 (ppb days)	13763	27470	2904
Nd120 (days)	29	18	-
MTDM (ppb)	53.9	54.7	39.6
Rural			
SOMO35 (ppb days)	39581	29101	2115
Nd120 (days)	134	4	-
MTDM (ppb)	63.8	52.9	38.9

3
 4
 5
 6
 7
 8
 9

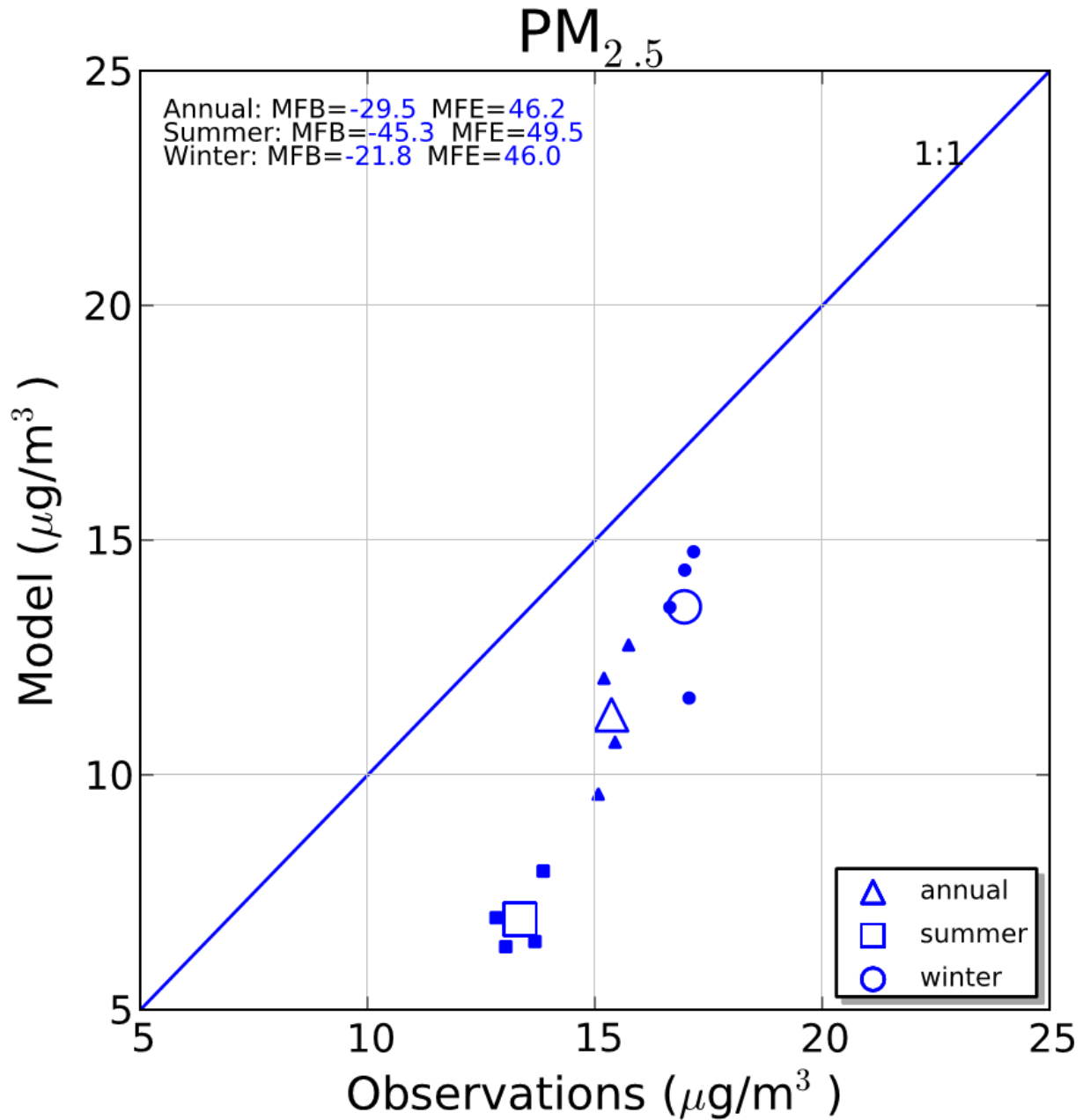


1 Figure 1. Local scale (IdF) simulation domain, with the city of Paris in the center (area enclosed
 2 in the purple line). Circles correspond to sites of the local air-quality monitoring network
 3 (AIRPARIF) with red for urban, blue for suburban and black for rural. Triangles correspond to
 4 the meteorological stations (the yellow triangle correspond to the Montsouris meteorological
 5 located in the city center).

6



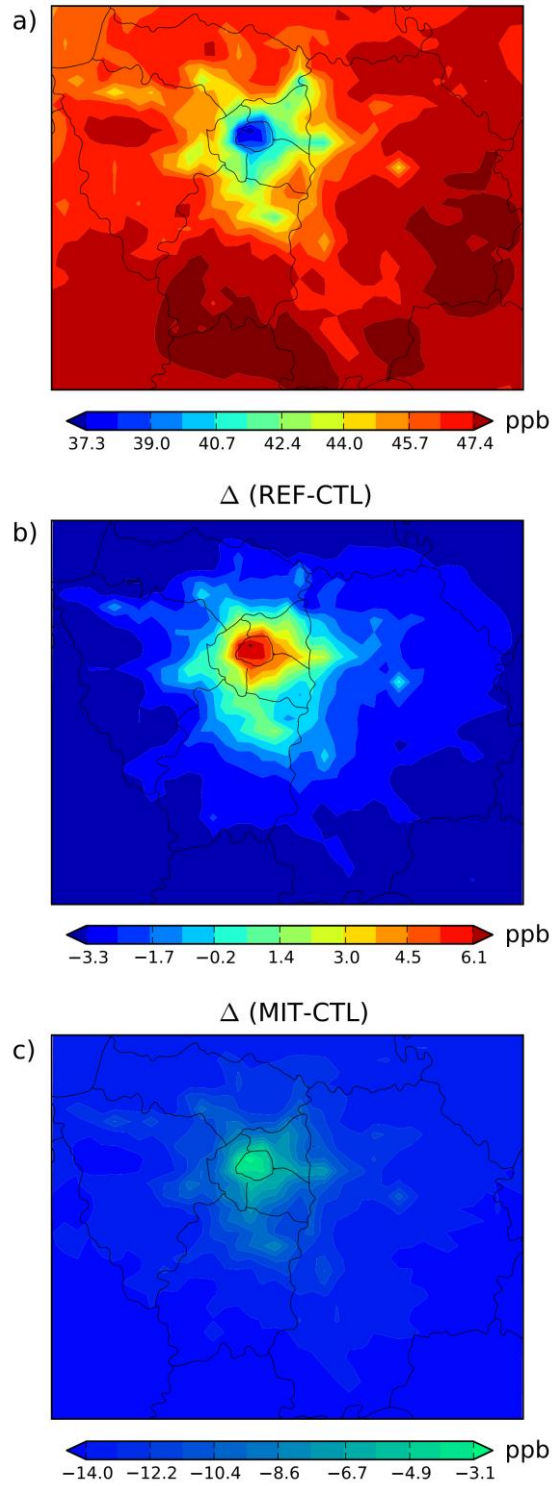
25 Figure 2. Scatter plots of mean daytime ozone (a) and O_x (b) during the April to August period
 26 from the model run against observations. Full small markers represent concentrations at
 27 individual stations while large hollow markers stand for the aggregated value. “Urban_max”
 28 stands for the daily maximum of an 8-hr running average.



1
 2 Figure 3. Scatter plot of mean daily PM_{2.5} from the model run during summer (JJA), winter
 3 (DJF) and on annual basis against observations. Full small markers represent concentrations at
 4 individual stations while large hollow markers stand for the aggregated value.

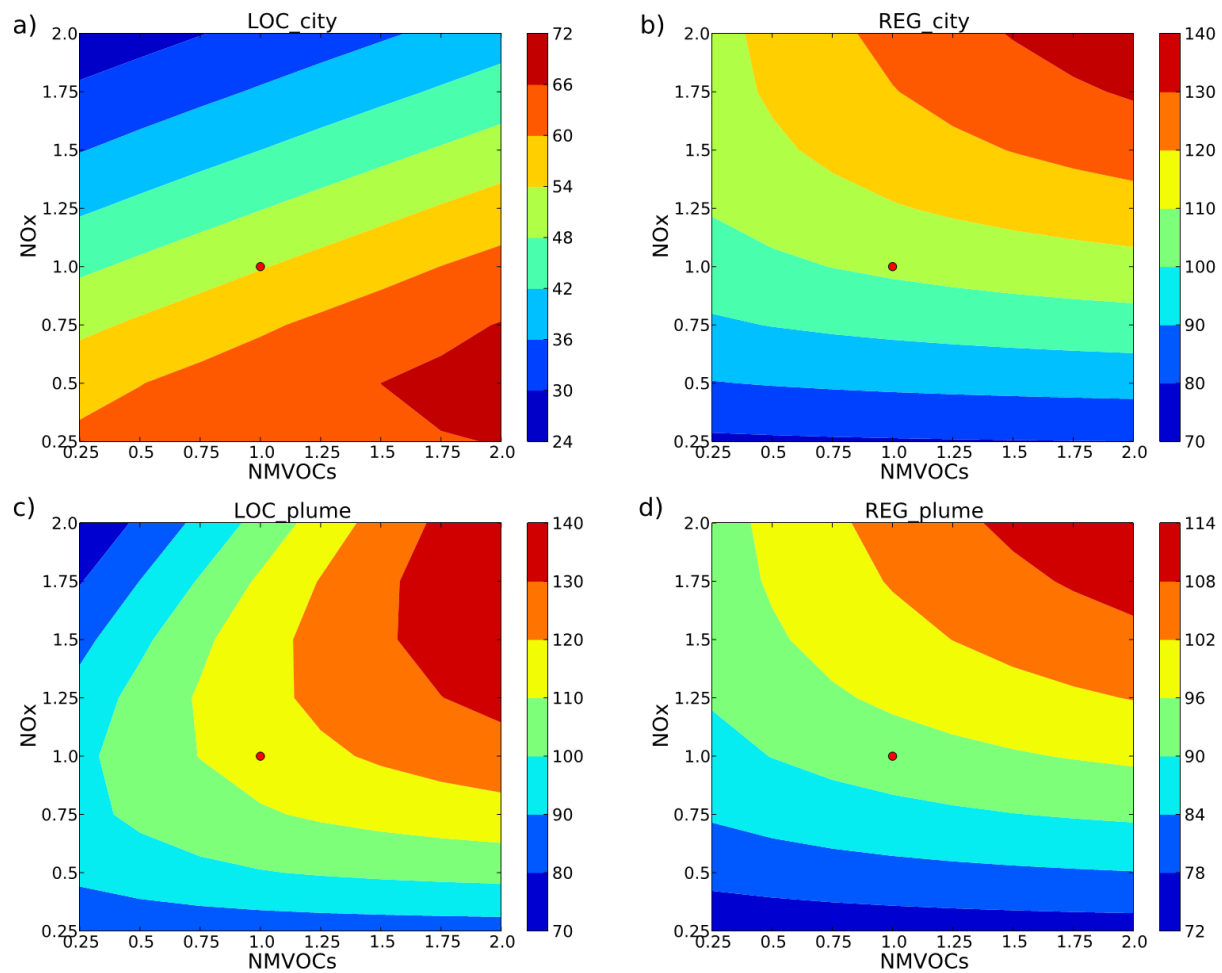
5
 6
 7
 8
 9

10yr mean of daily max O3 concentrations (APR-AUG)



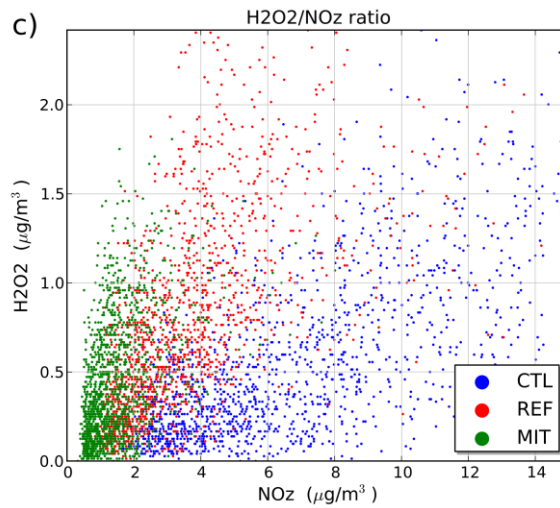
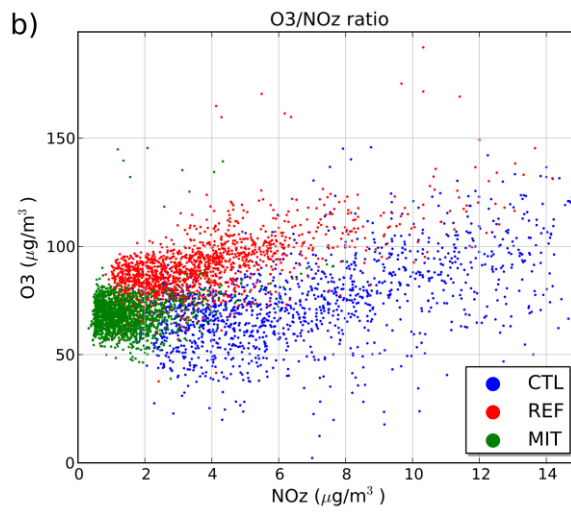
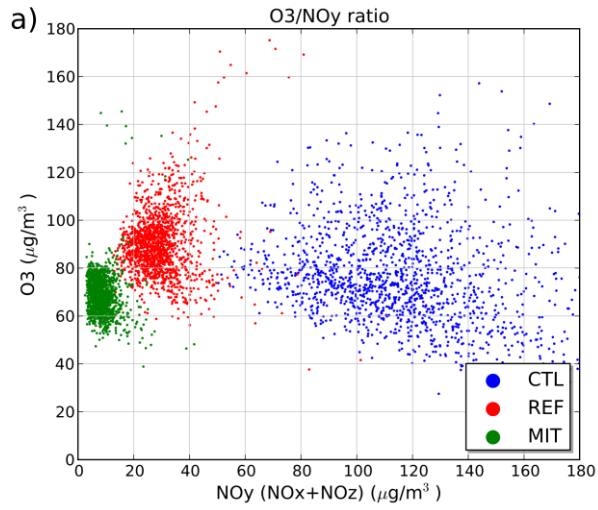
1
2 Figure 4. Present time ozone daily maximum (ppb) of 8-hr running means averaged over the
3 April-August period (a) and differences between the CTL run and the REF (b) and MIT
4 projections (c).

5



1
 2 Figure 5. Isocontours of maximum ozone concentrations over downtown Paris (top panels) and
 3 over the entire modelling domain (IdF) (bottom panels) as a function of ozone precursor
 4 emissions. Axis units are the coefficients of emission changes (in molecules/cm²/s) with respect
 5 to their baseline values (point 1.0, 1.0). Isopleths on the left are modelled with the LOC
 6 simulation and on the right with the REG simulation.

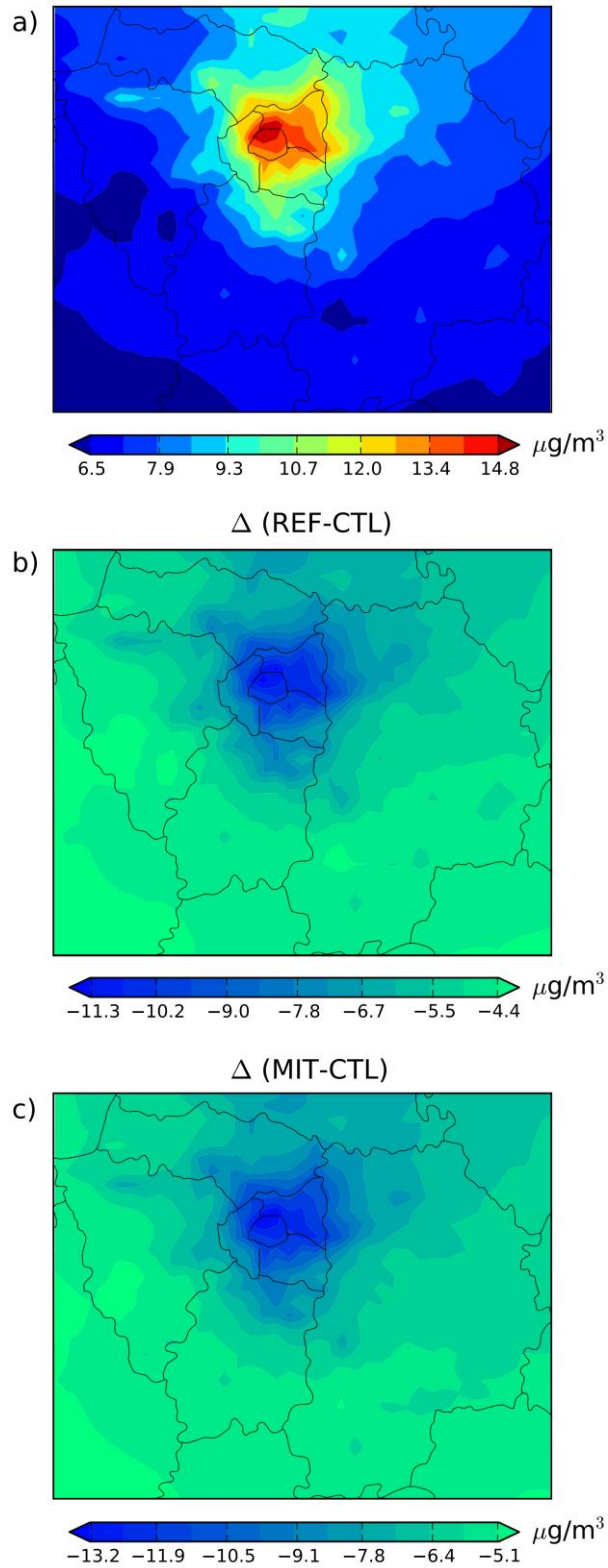
7
 8
 9



1
2
3
4
5
6
7
8
9
10
11
12
13
14
15
16
17
18
19
20
21
22
23
24
25
26
27
28
29
30
31

Figure 6. Ozone chemical regime indicators for the control run and the two future projections. Dots represent daily means averaged during the ozone period over the grid-cells of the downtown Paris area.

10yr mean of daily avg PM_{2.5} concentrations (DJF)



1
2 Figure 7. Wintertime (DJF) PM_{2.5} daily average fields ($\mu\text{g}/\text{m}^3$) for the control simulation (a) and
3 the differences between the latter and the REF (b) and MIT (c) future projections.